ELSEVIER

Int. J. Therm. Sci. 41 (2002) 447–454

International Journal of Thermal Sciences

www.elsevier.com/locate/ijts

Natural convection flow in a fluid-saturated porous medium enclosed by non-isothermal walls with heat generation

M. Anwar Hossain [a,*], Mike Wilson [b]

[a] *Department of Mathematics, University of Dhaka, Dhaka 1000, Bangladesh*
[b] *Department of Mechanical Engineering, University of Bath, Bath BA2 7AY, UK*

Received 31 May 2001; accepted 8 August 2001

Abstract

Unsteady laminar natural convection flow has been considered in a rectangular enclosure formed by non-isothermal walls, filled with a fluid-saturated porous medium and with internal heat generation. The top horizontal wall and right vertical wall of the enclosure are cold, the bottom wall is heated at a constant temperature and the left vertical wall is considered to be non-isothermal. The equations are non-dimensionalized and solved numerically by an upwind finite difference method together with a successive over-relaxation (SOR) technique. The effects of heat generation and the porosity of the medium on the streamlines and isotherms are presented, as well as on the rate of heat transfer from the walls of the enclosure. The fluid has Prandtl number $Pr = 0.7$ while the value of the Rayleigh number is 10^5. © 2002 Éditions scientifiques et médicales Elsevier SAS. All rights reserved.

Keywords: Heat generation; Natural convection flow; Fluid-saturated porous medium; Non-isothermal walls

1. Introduction

The characteristics of heat and fluid flow for a configuration of isothermal vertical walls, maintained at different temperatures and with adiabatic horizontal walls, are well understood (Ostrach [1,2]). Less work has been carried out for more complex thermal boundary conditions, such as an imposed thermal gradient that is neither purely horizontal nor purely vertical. Shiralkar and Tien [3] investigated, numerically, natural convection in an enclosure with temperature gradients imposed in both the horizontal and vertical directions simultaneously. A stabilizing vertical temperature gradient was found to result in lower vertical velocities and generation of secondary vortices at opposite corners. On the other hand, a destabilising vertical gradient leads to the destruction of stratification in the core and the formation of unstably stratified thermal layers adjacent to the upper and lower surfaces. Chao and Ozoe [4] investigated the problem of natural convection in an inclined box with half the bottom surface heated and half insulated, while the top surface was cooled. Anderson and Lauriat [5] analysed experimentally as well as theoretically the natural convection due to one isothermal cold vertical wall and a hot bottom wall. Kimura and Bejan [6] studied numerically the convection flow in a rectangular enclosure with the entire lower surface cooled and one of the vertical walls heated. November and Nansteel [7] and Nicolas and Nansteel [8] performed experiments and numerical investigations on convection in a water filled enclosure with a single cold isothermal vertical wall and a partially heated bottom wall. Granzarolli and Milanez [9] computed the case of a heated bottom wall and isothermally cooled vertical walls. Recently, Velusamy et al. [10] investigated the steady two-dimensional natural convection flow in a rectangular enclosure with a linearly-varying surface temperature on the left vertical wall, cooled right vertical and top walls and a uniformly-heated bottom wall. In this latter investigation, mild natural convection was found to reduce the heat load to the cold walls, and for any value of aspect ratio it was also found that there exists a critical Rayleigh number for which heat load is a minimum.

Here we investigate the problem posed by the above author [10] for an enclosure filled with a fluid-saturated porous medium, along with generation of heat depending on the fluid temperature. In recent years, flow in a confined porous medium has received considerable attention from experimentalists as well as theoreticians. This has importance for applications in developing technology and industry, such

* Correspondence and reprints.
E-mail address: anwar@udhaka.net (M.A. Hossain).

1290-0729/02/$ – see front matter
PII: S1290-0729(02)01337-6

Nomenclature

C_p	specific heat at constant pressure	$J\cdot kg^{-1}\cdot K^{-1}$	
Da	Darcy parameter		
g	gravitational acceleration	$m\cdot sec^{-2}$	
Ra	Rayleigh number		
H	enclosure hight	m	
k	effective thermal conductivity of the media	$W\cdot m^{-1}\cdot K^{-1}$	
K	permeability of the porous media	m^2	
p	fluid pressure	Pa	
Pr	Prandtl number		
t	time	s	
T	temperature	°C	
u	velocity in x-direction	$m\cdot s^{-1}$	
U_0	$= \nu/H$ reference velocity		
v	velocity in y-direction	$m\cdot s^{-1}$	
x, y	Cartesian coordinates	H	
X, Y	dimensionless coordinates		

Greek symbols

β	coefficient of thermal expansion of fluid	K^{-1}
θ	dimensionless temperature	
γ	porosity parameter $= 1/Da$	
λ	dimensionless heat absorption/generation parameter	
μ	effective dynamic viscosity	$Pa\cdot s^{-1}$
ν	effective kinematic viscosity $= \mu/\rho$	
ρ	fluid density at reference temperature T_c	
τ	dimensionless time	
ψ	streamfunction	$m^2\cdot s^{-1}$
Ω	dimensionless vorticity	

as prevention of sub-oil water pollution, storage of nuclear waste and geothermal energy systems (for which Cheng [11] provides an extensive review).

In early works on flow in porous media, the Darcy law has been used which is applicable to slow flows and does not account for inertial and boundary effects (termed as non-Darcy effects). These effects are important when the flow velocity is relatively high and in the presence of a boundary, as reported first by Vafai and Tien [12]. Recently, Khanafer and Chamkha [13] investigated numerically the Brinkman-extended Darcy unsteady mixed convection flow in an enclosure, with internal heat generation and with inclusion of the convective terms in the governing equations, by using the control volume method developed by Patankar [14].

A detailed development of the present investigation is given in the subsequent sections.

2. Mathematical formulation

Consider a rectangular enclosure of height H filled with a fluid-saturated porous medium as shown in Fig. 1. The right and the top walls are maintained at a constant cold temperature T_C. The temperature of the left wall is T_H at the bottom and reduces linearly to T_C at the top. The bottom wall of the enclosure is isothermal at T_H. The boundary condition at the right bottom corner deserves some explanation. In the reactor on which this model is based, a small gap of height h (5–10 mm) between the bottom and the right walls is filled with a sodium deposit. The temperature in the gap is expected to vary linearly from T_H to T_C over a small non-dimensional distance d. We also bring into account the effect of temperature-dependent heat generation in the flow

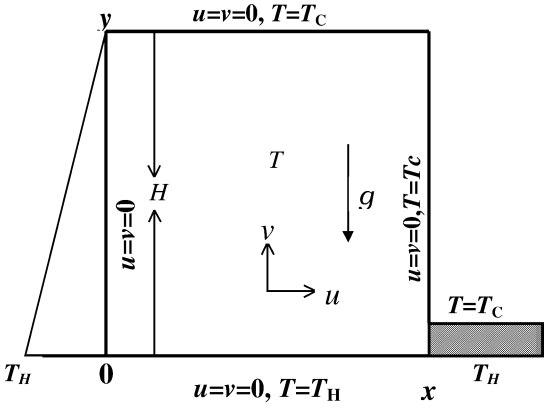

Fig. 1. The flow configuration and coordinate system.

region. The volumetric rate of heat generation, q''' [$W\cdot m^{-3}$], is assumed to be:

$$q''' = \begin{cases} Q_0(T - T_C), & T \geqslant T_C \\ 0, & T < T_C \end{cases} \tag{1}$$

where Q_0 is the heat generation constant. The above relation, as explained by Vajravelu and Hadjinicolaou [15], is valid as an approximation of the state of some exothermic process, which means that heat flows from the surface to the enclosure.

We further assume unsteady laminar flow of a viscous incompressible fluid having constant properties. The effect of buoyancy is included through the well-known Boussinesq approximation. Finally, the direction of the gravitational force is as indicated in Fig. 1.

Under the above assumptions, the conservation equations for mass, momentum and energy in a two-dimensional Cartesian co-ordinate system are:

$$\frac{\partial u}{\partial x} + \frac{\partial v}{\partial y} = 0 \tag{2}$$

$$\frac{\partial u}{\partial t}+u\frac{\partial u}{\partial x}+v\frac{\partial u}{\partial y} = -\frac{1}{\rho}\frac{\partial p}{\partial x}+\nu\left(\frac{\partial^2 u}{\partial x^2}+\frac{\partial^2 u}{\partial y^2}\right)-\frac{\nu}{K}u \quad (3)$$

$$\frac{\partial v}{\partial t}+u\frac{\partial v}{\partial x}+v\frac{\partial v}{\partial y} = -\frac{1}{\rho}\frac{\partial p}{\partial y}+\nu\left(\frac{\partial^2 v}{\partial x^2}+\frac{\partial^2 v}{\partial y^2}\right)-\frac{\nu}{K}v+g\beta_{\mathrm{T}}(T-T_{\mathrm{C}}) \quad (4)$$

$$\frac{\partial T}{\partial t}+u\frac{\partial T}{\partial x}+v\frac{\partial T}{\partial y} = \alpha\left(\frac{\partial^2 T}{\partial x^2}+\frac{\partial^2 T}{\partial y^2}\right)+\frac{Q_0}{\rho C_{\mathrm{p}}}(T-T_{\mathrm{C}}) \quad (5)$$

where u and v are the fluid velocity components in the x- and y-direction, respectively. T is the time, p is the fluid pressure, β is the volumetric thermal expansion coefficient, K is the permeability of the porous medium, and ρ, α and C_{p} are, respectively the density of the fluid, the thermal diffusivity and the specific heat at constant pressure. In the present investigation, porous medium inertia effects have been neglected in the momentum equations, and the effects of viscous dissipation are neglected from the energy equation.

In Eqs. (3) and (4) K is the measure of the permeability of the porous medium (a packed bed of spheres), defined by

$$K=\frac{\varepsilon^{+3}}{180(1-\varepsilon^{+})^2}d^2 \quad (6a)$$

where, d is the diameter of the solid sphere and ε^{+} is known as the porosity of the media and is defined by

$$\varepsilon^{+}=\frac{V_{\mathrm{f}}}{V_{\mathrm{c}}} \quad (6b)$$

Here V_{f} is the volume of the fluid and V_{c} is the control volume.

The following dimensionless variables are constructed:

$$X=\frac{x}{H}\qquad Y=\frac{y}{H}\qquad \tau=\frac{tU_0}{H}$$
$$U=\frac{u}{U_0}\qquad V=\frac{v}{U_0}\qquad \theta=\frac{T-T_{\mathrm{C}}}{T_{\mathrm{H}}-T_{\mathrm{C}}} \quad (7)$$

Introducing the above dimensionless dependent and independent variables in the governing Eqs. (3)–(5) the following equations are obtained:

$$\frac{\partial \Omega}{\partial \tau}+\frac{\partial(U\Omega)}{\partial X}+\frac{\partial(V\Omega)}{\partial Y} = \left(\frac{\partial^2}{\partial X^2}+\frac{\partial^2}{\partial Y^2}-\gamma\right)\Omega+\frac{Ra}{Pr}\frac{\partial\theta}{\partial X} \quad (8)$$

$$\frac{\partial \theta}{\partial \tau}+\frac{\partial(U\theta)}{\partial X}+\frac{\partial(V\theta)}{\partial Y} = \frac{1}{Pr}\left(\frac{\partial^2}{\partial X^2}+\frac{\partial^2}{\partial Y^2}+Pr\,\lambda\right)\theta \quad (9)$$

where

$$\Omega=-\left(\frac{\partial^2}{\partial X^2}+\frac{\partial^2}{\partial Y^2}\right)\psi \quad (10)$$

is the vorticity function and ψ is the stream function defined by:

$$U=\frac{\partial\psi}{\partial Y},\qquad V=-\frac{\partial\psi}{\partial X} \quad (11)$$

In the above equations

$$Ra=\frac{g\beta_{\mathrm{T}}(T_{\mathrm{H}}-T_{\mathrm{C}})H^3}{\alpha\nu},\qquad Pr=\frac{\nu}{\alpha},$$
$$\gamma=1/Da=\frac{H^2}{K},\qquad \lambda=\frac{Q_0H^2}{\rho\nu C_{\mathrm{p}}} \quad (12)$$

The dimensionless initial and boundary conditions are:

$$\begin{array}{ll} U=V=\theta=0 & \text{for } \tau=0 \\ U=V=0 & \text{for } 0\leqslant Y\leqslant 1 \text{ at } X=1 \\ U=V=\theta=0 & \text{for } 0\leqslant X\leqslant 1 \text{ at } Y=1 \\ U=V=0,\quad \theta=1 & \text{for } 0\leqslant X\leqslant 1 \text{ at } Y=0 \\ \theta=1-Y & \text{for } 0\leqslant Y\leqslant 1 \text{ at } X=0 \\ \theta=1-Y/L & \text{for } 0\leqslant Y\leqslant L \quad \text{and} \\ \theta=0 & \text{for } L<Y\leqslant 1 \text{ at } X=1 \end{array} \quad (13)$$

where L is the width of the gap near the bottom-right corner.

An upwind finite-difference method, together with a successive over-relaxation (SOR) iteration technique has been employed to integrate the model Eqs. (7) and (8) governing the flow. It is clear that the non-dimensional parameters of interest are the Rayleigh number, Ra, the Prandtl number, Pr, the porosity parameter, $\gamma(=1/Da)$, and the heat generation number, λ. In the present investigation, pertaining to argon gas, the value of the Prandtl number is chosen as 0.7 and the Rayleigh number is taken to be 10^5. The aspect ratio considered is unity and the value of $h=1/(n-1)$, n is the number of grid points in the Y direction) is 0.02.

The corresponding problem for pure fluid without the effect of heat-generation has been investigated by Velusamy et al. [10] using the control volume method for different values of the Rayleigh number and two values of the aspect ratio (1 and 2), also for $Pr=0.7$.

Once we know the numerical values of the temperature function we may obtain the rate of heat flux from each of the walls. The non-dimensional heat flux from any surface is given by $-(\partial T/\partial n)$, where n is the direction normal to the wall. For example, the non-dimensional heat transfer rate, q, per unit length in the depthwise direction for the left vertical surface is:

$$q=-\int_0^1\left(\frac{\partial T}{\partial X}\right)_{X=0}\mathrm{d}Y \quad (14)$$

The results shown and discussed in the following section have been calculated from zero initial velocities and mean values of temperature. A grid dependence study has been

Table 1
Comparison of numerical values of stream-function against different meshes for $Ra = 10^5$ and $Pr = 0.7$

Meshes	$h = 1/(n-1)$	ψ_{max}	ψ_{min}
41×41	1/40	0.807008	−34.6537
51×51	1/50	0.813292	−34.97759
61×61	1/60	0.812256	−35.23735

carried out for a thermally-driven cavity flow for the above mentioned parameter values with meshes of 41×41, 51×51 and 61×61 points, and resulting flow quantities are listed in Table 1. For computational economy, a 51×51 mesh has been used throughout for the simulations described below. With this mesh, for the case with $\lambda = \gamma = 0$, $Pr = 0.7$ and $Ra = 10^5$, the maximum and minimum values of ψ were found to be 0.81 and −34.98. The corresponding values obtained by Velusamy et al. [10] using the control volume method are 0.85 and −34.95. Thus the present results agree sufficiently well with the previous solution. Finally, simulations were carried out until steady state solutions were obtained.

3. Results and discussions

Numerical results for natural convection heat transfer for a heat-generating fluid in a rectangular cavity filled with a saturated porous medium with uniform porosity are described, subject to a non-uniformly heated left wall and heated bottom wall. As mentioned above, the non-dimensional controlling parameters are the Rayleigh number, *Ra*, the Prandtl number, *Pr*, the porosity parameter, γ ($= 1/Da$) and the heat generation parameter, λ. In the absence of heat generation and for a pure fluid ($\gamma = 0.0$) the effect of Rayleigh number for a rectangular cavity with aspect ratio in the range 1 to 5 has been investigated by Velusamy et al. [10], for fluid having $Pr = 0.7$. Here therefore we have used fixed values of Pr ($= 0.7$), Rayleigh number Ra ($= 10^5$) and aspect ratio ($= 1$) and have obtained solutions for different values of the porosity parameter, γ, and the heat generation parameter, λ.

We first show the streamlines and isotherms for values of λ equal to 0.0, 10.0 and 20.0 in Figs. 2–4. Fig. 2 shows the streamlines and isotherms for the case studied by Velusamy et al. [10]. Now comparing Figs. 3(a) and 4(a) we see that the size of the secondary cell that develops at the left top corner increases with increasing value of the heat generation parameter. It may further be seen that the value of ψ_{max} also increases as λ increases. Also, for non-zero values of λ, the centre of the primary vortex moves towards the bottom right corner and the magnitude of ψ_{min} decreases considerably. It may be anticipated that further increase of the heat generation parameter would create two vortices of equal strength.

In Fig. 2(b) it can be seen that the isotherms are clustered close to the bottom surface, which points to the existence of steep temperature gradients in the vertical direction in this region. In the bulk of the cavity, away from this localized area, the temperature gradients are weak. Comparing Figs. 3(b) and 4(b) with Fig. 2(b) it can be seen that in the presence of heat generation and for increasing value of the heat generation parameter, λ, the region of clustered isotherms moves to the right and towards the top cold surface of the enclosure. The temperature gradient in the middle of the cavity also appears to increase. It may also be expected that further increase of the heat generation parameter will force the isotherms to become clustered in the region near the top surface.

The effects of internal heat generation on the rate of heat transfer from the sidewalls are illustrated in Fig. 5. In these figures all the curves for $\lambda = 0$ are for the flow of a pure fluid in the absence of internal heat generation, and agree qualitatively with the results of Velusamy et al. [10]. In Fig. 5(a) we see that the rate of heat transfer from the heated bottom surface decreases with increase in the value of the heat generation parameter. This is expected, since the heat

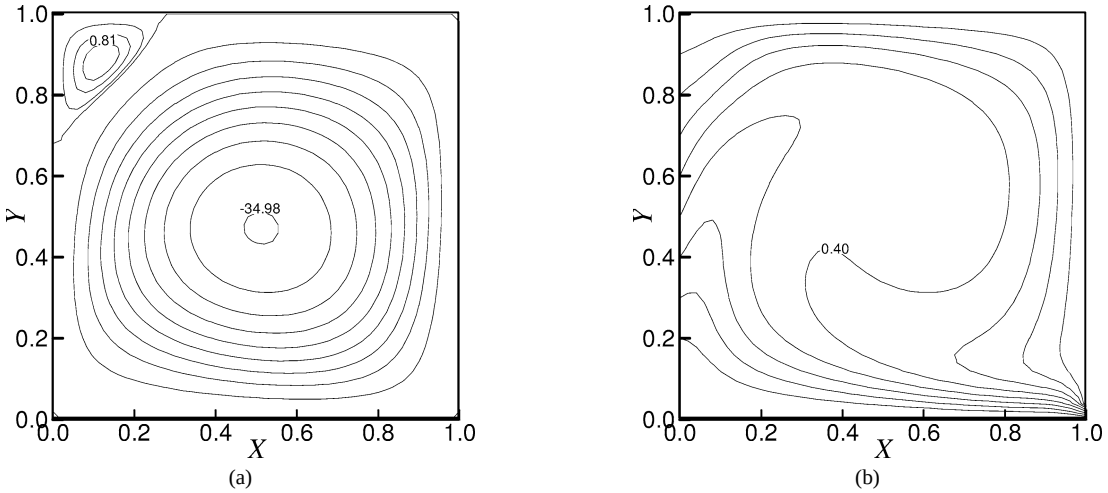

(a) (b)

Fig. 2. (a) Streamlines and (b) Isotherms for $\lambda = 0.0$ while $Ra = 10^5$, $Pr = 0.7$ and $\gamma = 0.0$.

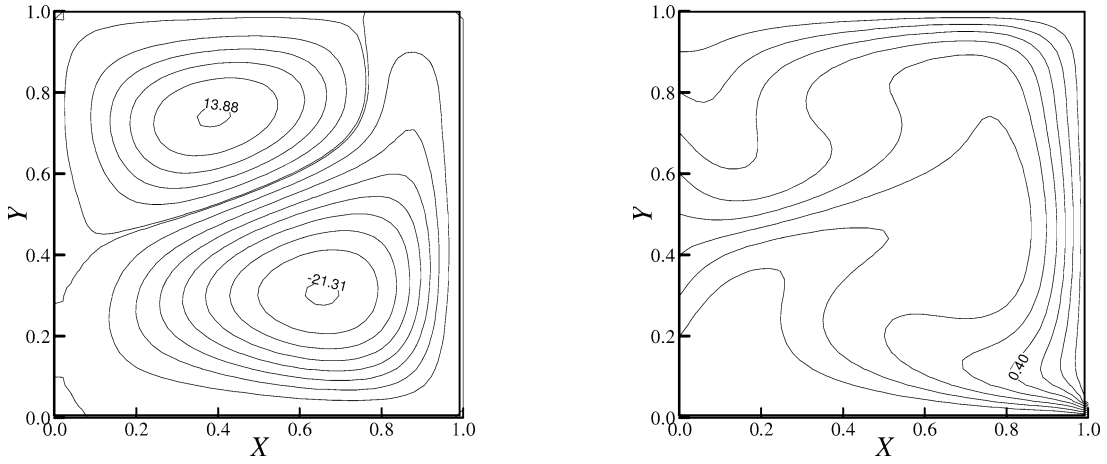

Fig. 3. (a) Streamlines and (b) Isotherms for $\lambda = 10.0$ while $Ra = 10^5$, $Pr = 0.7$ and $\gamma = 0.0$.

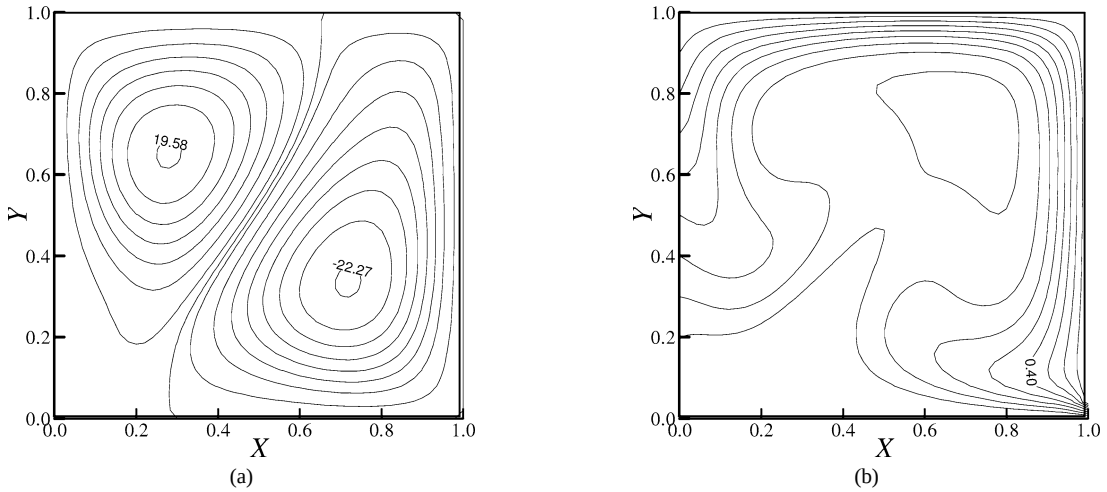

Fig. 4. (a) Streamlines and (b) Isotherms for $\lambda = 20.0$ while $Ra = 10^5$, $Pr = 0.7$ and $\gamma = 0.0$.

generation mechanism will increase the fluid temperature near the bottom surface, resulting in increased resistance to the transfer of heat in the verical direction. The heat transfer distribution for the top wall is shown in Fig. 5(b). The top corner regions are inactive zones and heat transfer is mainly by conduction. For all values of the heat generation parameter, the flux of heat is unity at the left end and zero at the right end due to the boundary conditions. In between there is a peak value, where fluid issuing from near the left wall meets the top surface. This peak value increases with increasing addition of heat due to heat generation phenomena. Now we look to Fig. 5(c) for the effect of heat generation on the heat flux from the left wall, the temperature of which increases linearly with height from the bottom to the top. Looking at the distribution corresponding to $\lambda = 0$, it can be seen that there exists one full wave pattern with one maximum and one minimum. A similar pattern can be observed when $\lambda = 10.0$, with the difference that for the first part of the surface the heat flux is lower and for the remainder is higher than for $\lambda = 0$. We further observe that a double trough develops in the heat flux distribution for the highest value of λ. Finally, Fig. 5(d) shows the effect of the heat generation parameter on the heat–flux from the right wall of the enclosure. The heat transfer at the bottom of the wall is purely due to conduction and, for $Y < L$ $(= 0.1)$, the heat flux is high for all values of λ. A local minimum in the heat flux distribution develops in the region $0.1 < Y < 0.3$ for all values of λ. The local maximum in the heat flux for $Y > 0.3$ increases with increase of the heat generation parameter.

Now, we discuss the effect of the porosity of the medium on the streamlines and isotherms through Figs. 6–8. The figures show results for values of $\gamma = 10.0$, 20, and 30 but in the absence of heat generation in the flow. Comparing Figs. 6(a)–8(a) it can be seen that the volume flow rate in the primary as well as in the secondary vortex regimes decreases as γ increases, as the resistance to fluid flow increases. (The flow-rate would become much higher at porosity values closer to zero.) Figs. 6(b)–8(b) show the effect of this increasing resistance on the temperature distributions.

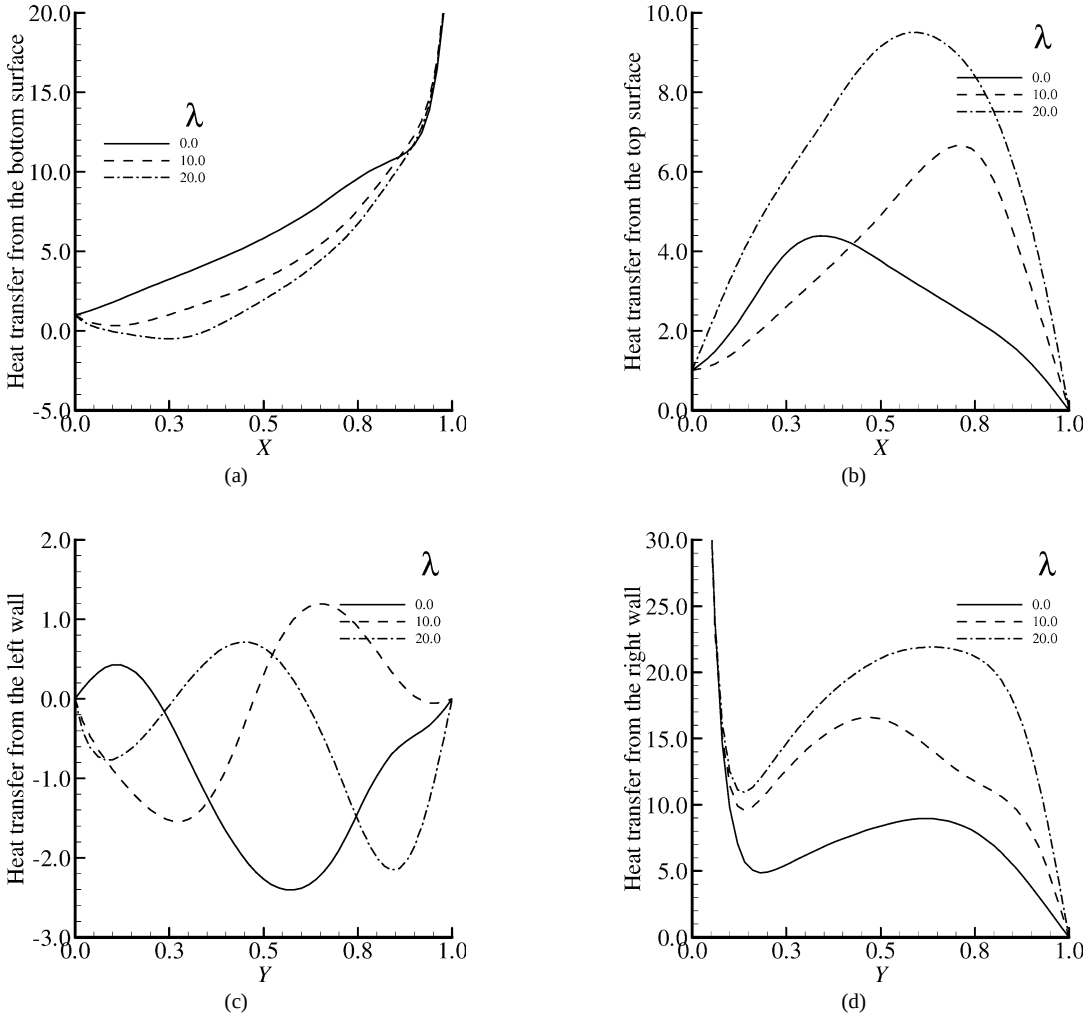

Fig. 5. Rate of heat transfer from the side walls for different values of λ while $Ra = 10^5$, $Pr = 0.7$, $\gamma = 0.0$ (a) bottom wall, (b) topsurface, (c) left wall and (d) right wall.

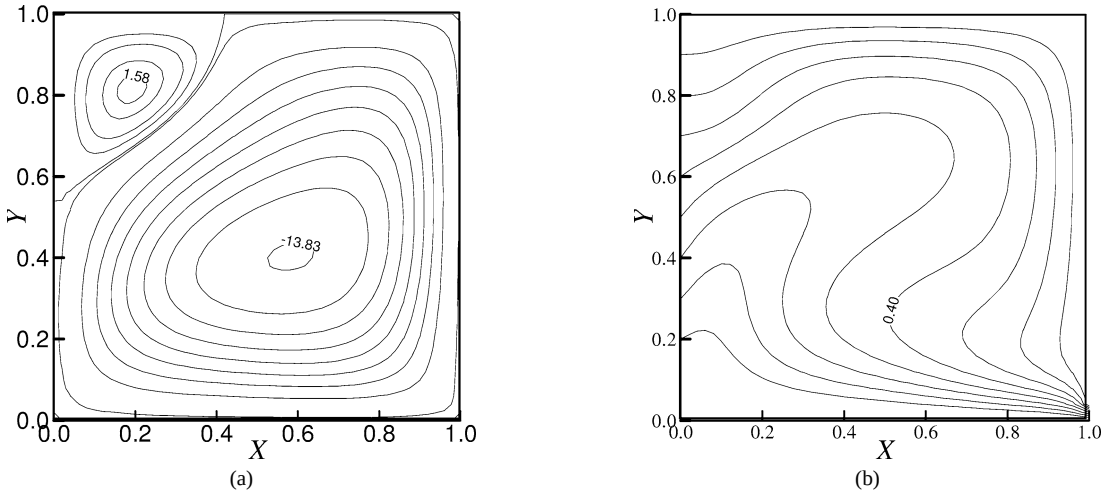

Fig. 6. (a) Streamlines and (b) Isotherms for $\gamma = 10.0$ while $Ra = 10^5$, $Pr = 0.7$ and $\lambda = 0.0$.

Now we discuss the effect of the porosity of the medium on the heat transfer from the walls of the enclosure, again in the absence of heat generation. In Figs. 9(a)–(d) we display the heat–flux distributions for values of the porosity parameter $\gamma = 0.0$, 10.0, 20.0 and 30.0, for $Pr = 0.7$ and $Ra = 10^5$. From these figures it can be seen that, as the value

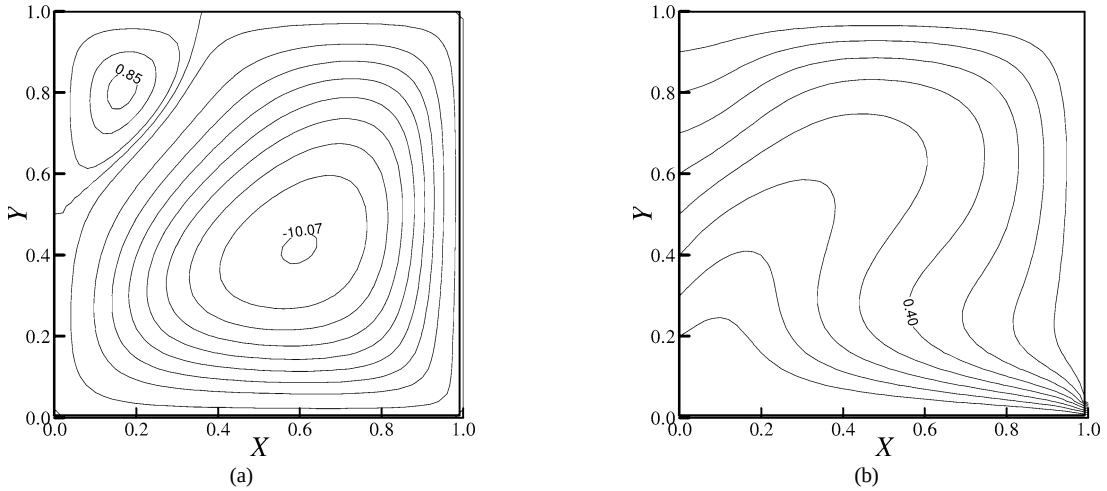

Fig. 7. (a) Streamlines and (b) Isotherms for $\gamma = 20.0$ while $Ra = 10^5$, $Pr = 0.7$ and $\lambda = 0.0$.

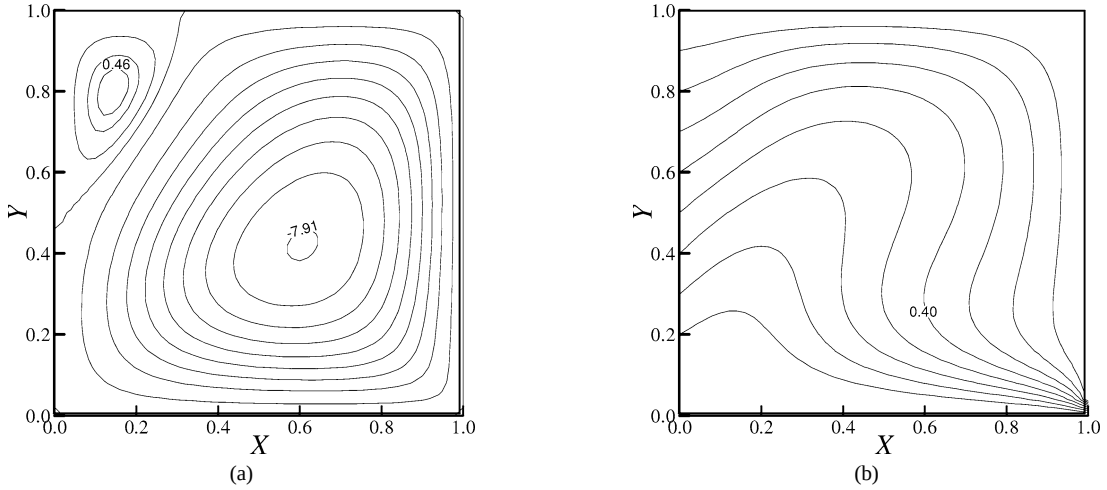

Fig. 8. (a) Streamlines and (b) Isotherms for $\gamma = 30.0$ while $Ra = 10^5$, $Pr = 0.7$ and $\lambda = 0.0$.

of the porosity parameter increases, the heat transfer from the bottom wall decreases, Fig. 9(a), and the peak value of heat transfer also decreases with increasing γ at the top and right walls. For the linearly-varying temperature left wall, the heat flux is lower near the bottom and higher near the top for the cases with $\gamma > 0$ than for the pure fluid case ($\gamma = 0$), and a limiting distribution of (comparatively low) heat transfer is approached as γ increases.

4. Conclusions

We have investigated numerically the separate effects of heat generation in a fluid and the porosity of the medium on the natural convection laminar flow and heat transfer in an enclosure with non-isothermal walls, using a finite-difference solution technique and with buoyancy effects treated using the Boussinesq approximation. The studies have been carried out for a fluid having Prandtl number 0.7 and for a Rayleigh number of 10^5. For the case of a pure fluid (i.e., flow in a non-porous medium) without heat generation the solutions are in agreement with other results published in the literature.

The top horizontal wall of the enclosure is cold and the bottom wall is heated. Increasing heat generation in the fluid (as a function of the local fluid temperature) reduces thermal gradients near the heated bottom wall of the enclosure, leading to higher gradients (and thus higher surface heat flux) at the cold top and right walls. The strength of the dominant vortex induced by bouyancy is reduced due to increasing internal heat generation, and a more nearly equal double vortex structure develops. Increasing the porosity of the medium (in the absence of heat generation) reduces the volume flow rate of fluid in the dominant vortex and leads to a general reduction in heat transfer at the walls.

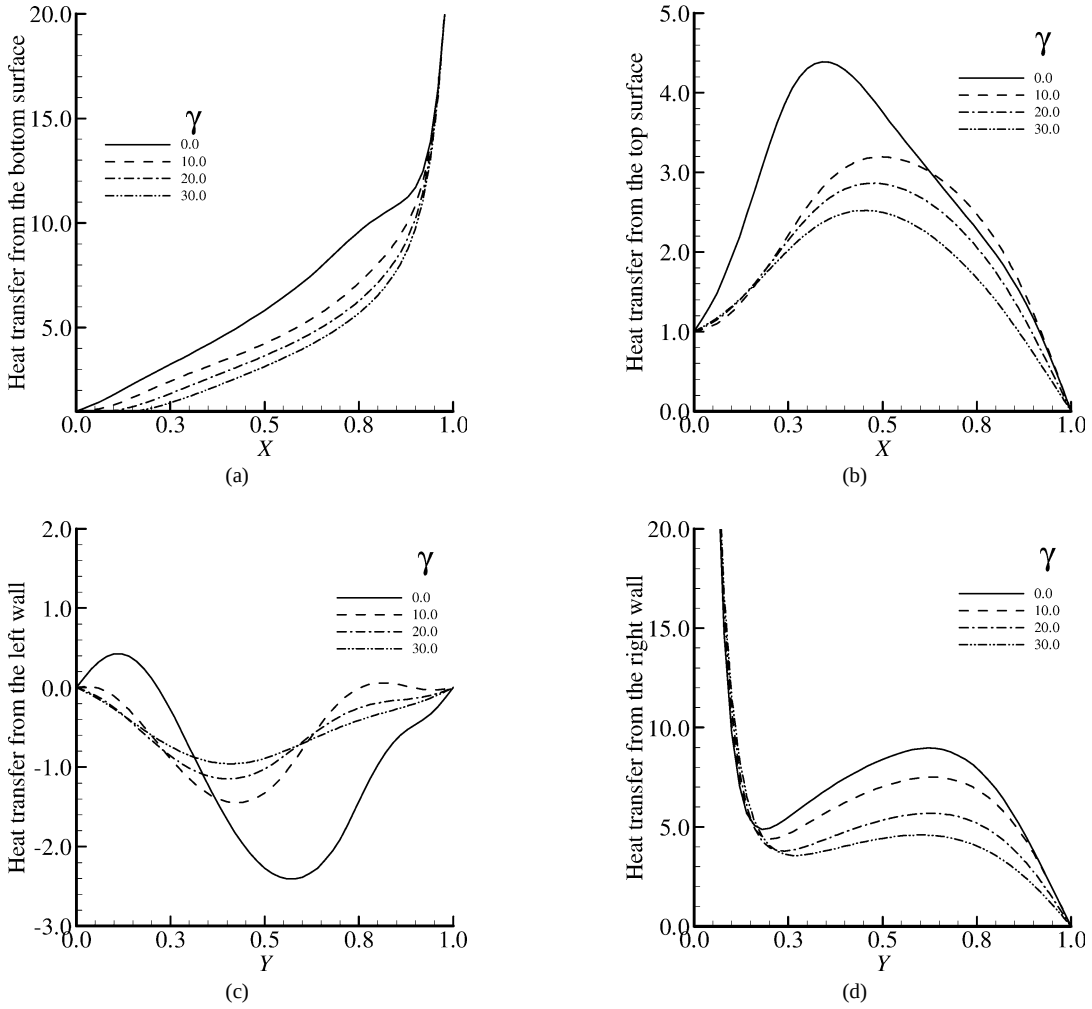

Fig. 9. Rate of heat transfer from the side walls for different values of γ while $Ra = 10^5$, $Pr = 0.7$, $\lambda = 0.0$ (a) bottom wall, (b) topsurface, (c) left wall and (d) right wall.

Acknowledgement

One of the authors (MAH) acknowledges with gratitude the Ministry of Science and Technology, Peoples Republic of Bangladesh, for providing funds to perform this work (Grant No. BPM/Sec-9/B/Gr 2000-2001/463).

References

[1] S. Ostrach, Natural convection in enclosures, in: J.P. Hartnett, H. Irving (Eds.), Adv. Heat Transfer 8 (1972) 161–227.
[2] S. Ostrach, Natural convection in enclosures, ASME J. Heat Transfer 110 (1988) 1175–1190.
[3] G. Shiralkar, C. Tien, A Numerical study of the effect of a vertical temperature difference imposed on a horizontal enclosure, Numer. Heat Transfer 5 (1982) 185–197.
[4] P. Chao, H. Ozoe, Laminar natural convection in an inclined rectangular box with lower surface half-heated and half insulated, ASME J. Heat Transfer 105 (1983) 425–432.
[5] R. Anderson, G. Lauriat, The horizontal natural convection boundary layer regime in a closed cavity, in: Proc. 8th Internat. Heat Transfer Conf., San Francisco, California, USA, 1986, pp. 1453–1458.
[6] S. Kimura, A. Bejan, Natural convection in differentially heated corner region, Phys. Fluids 28 (1985) 2980–2989.
[7] M. November, M.W. Nansteel, Natural convection in a rectangular enclosure heated from below and cooled along one surface, Internat. J. Heat Mass Transfer 30 (1987) 2433–2440.
[8] J.D. Nicolas, M.W. Nansteel, Natural convection in a rectangular enclosure with partial heating on the lower surface; experimental results, Internat. J. Heat Mass Transfer 36 (1993) 4067–4071.
[9] M.M. Ganzarolli, L.F. Milanez, Natural convection in rectangular enclosures heated from below and symmetrically cooled from the sides, Internat. J. Heat Mass Transfer 38 (1995) 1063–1073.
[10] K. Velusamy, T. Sundarajan, K.N. Seetharamn, Laminar natural convection in an enclosure formed by non-isothermal walls, in: Proc. 11th Internat. Conf. Heat Transfer, Korea, Vol. 3, 1998, pp. 459–464.
[11] P. Cheng, Heat transfer in geothermal systems, Adv. Heat Transfer 4 (1978) 1–105.
[12] K. Vafai, C.L. Tien, Boundary and inertia effects on flow and heat transfer in porous media, Internat. J. Heat Mass Transfer 24 (1981) 195–203.
[13] K.M. Khanafer, A.J. Chamkha, Mixed convection flow in a lid-driven enclosure filled with a fluid-saturated porous media, Internat. J. Heat Mass Transfer 42 (1999) 2465–2481.
[14] S.V. Patankar, Numerical Heat Transfer and Fluid Flow, Hemisphere, Washington, DC, 1980.
[15] K. Vajravelu, A. Hadjinicolaou, Convective heat transfer in an electrically conducting fluid at a stetching surface with uniform free stream, Internat. J. Engrg. Sci. 34 (1997) 1237–1244.